Electronic Supplementary Material (ESI) for ChemComm.

Supporting Information

From a layered iridium(III)-cobalt(II)-organophosphonate to an efficient oxygen-evolution-reaction electrocatalyst

Chwen-Haw Liao[+,a] Fan Kun[+,a] Song-Song Bao,[a] Hao Fan,[b] Xi-Zhang Wang,[b] Zheng Hu,[b] Mohamedally Kurmoo,[c] and Li-Min Zheng [a,*]

[a] *State Key Laboratory of Coordination Chemistry, Coordination Chemistry Institute, School of Chemistry and Chemical Engineering, Nanjing University, Nanjing 210093, P. R. China; E-mail:* lmzheng@nju.edu.cn
[b] *Key Laboratory of Mesoscopic Chemistry of MOE, School of Chemistry and Chemical Engineering, Nanjing University, Nanjing 210023, P. R. China*
[c] *Université de Strasbourg, Institut de Chimie de Strasbourg, CNRS-UMR7177, 4 rue Blaise Pascal, Strasbourg Cedex 67070, France.*

Experimental section

Chemicals. All starting materials including cobalt nitrate hexahydrate ($Co(NO_3)_2\cdot 6H_2O$), N,N'-dimethylformamide (DMF), hydrochloric acid (HCl), IrO_2 (Alfa-Aesar, 99%), and Co_3O_4 (Alfa-Aesar, 99%) were of reagent grade quality obtained from commercial sources and used without further purification. Ir(ppy-COOH)$_3$ and *R*-(1-phenylethylamine)methylphosphonic acid (*R*-pempH$_2$) were prepared according to procedures reporting in the literature.[1,2]

Synthesis of $Co^{II}_2[Ir^{III}(ppy\text{-}COOH)_2(ppy\text{-}COO)]_2(HOCH_2PO_3)\cdot 12H_2O\cdot 2.5DMF$ (1). To a mixture of *R*-pempH$_2$ (0.06 mmol) and $Co(NO_3)_2\cdot 6H_2O$ (0.05 mmol) in 2 mL deionized water was added a solution of Ir(ppy-COOH)$_3$ (0.015 mmol) in 2 mL DMF. The mixture solution was poured into a 5 mL glass bottle, and 23 μL HCl (12 M) was added into the mixture. The glass was sealed and heated at 100^{o}C for 96 h. After cooling, red hexagonal crystals of **1** were collected as a single phase, washed with DMF and ethanol, and dried under vacuum for 24 h. Elemental analyses calcd (%) for $C_{80.5}H_{90.5}N_{8.5}O_{30.5}Co_2Ir_2$: C, 43.98; H, 4.15; N, 5.42 %; found: C, 42.91; H, 4.01; N, 5.48 %. IR (KBr, cm^{-1}): 3360(w), 2922(w), 2779(w), 2368(w), 1654(s), 1581(s), 1555(m), 1519(w), 1467(w), 1355(s), 1263(w), 1224(w), 1213(w), 1164(w), 1098(m), 1022(m), 965(w), 883(w), 827(w), 773(s), 692(w), 657(w), 636(w).

Preparation of mixed-IrO_2/Co_3O_4. The mixed-IrO_2/Co_3O_4 sample was prepared by mixing 3.68 mg IrO_2 with 1.31 mg Co_3O_4. The mole ratio of IrO_2 and Co_3O_4 is 3:1.

Characterization. The single crystal diffraction data of 1 were collected using a Bruker SMART APEX II diffractometer equipped with monochromatic Mo-Kα radiation (λ =0.71073 Å) at 123 K. The structure was solved by direct method and refined on F^2 by full-matrix least-squares using SHELXTL. The PXRD data are recorded on a Bruker D8 ADVANCE X-ray powder diffractometer (CuKα) at room temperature.

Scanning Electron Microscope (SEM) images were performed on a SHIMADZU SSX-550. Transmission electron microscopic (TEM) images were obtained on a JEM-2800 transmission electron microscope (JEOL Ltd., Japan). IR spectra were measured by transmission through KBr pellets on a Bruker Tensor 27 spectrometer in the range 400 - 4000 cm^{-1}. Thermogravimetric analyses were performed in nitrogen in the range 25 to 600 °C at a heating rate of 5 °C min^{-1} on METTLER TOLEDO TGA/DSC instrument. Elemental analyses for C, H and N were determined with a PerkinElmer 240C elemental analyzer. Adsorption/desorption isotherms were measured by using a BELSORP-max instrument (BEL Japan, Inc.). The UV/Vis and luminescence spectra were recorded on PerkinElmer Lambda 950 UV/Vis/NIR and PerkinElmer LS55 fluorescence spectrometers, respectively, at room temperature. The Adsorption/desorption isotherms were measured by using a BELSORP-max instrument (BEL Japan, Inc.).

Electrochemical measurements. The electrochemical tests including cyclic voltammetry (CV) and rotating disk electrode (RDE) voltammetry were performed on an MSR electrode rotator (Pine Instrument Co.) coupled with a CHI 760C workstation (CH Instruments) with the counter electrode of Pt wire for OER using Ag/AgCl (3 M KCl) as reference electrode. The homogenous catalyst inks were prepared by adding 5 mg of **1@600** powder to a mixture of 0.80 mL deionized water, 0.20 mL ethanol, and 50 µL Nafion (Alfa, 5 wt %) followed by 30 min ultrasonic treatment. A 10 µL portion of fresh catalyst ink was dropped onto a glassy-carbon electrode (GC: 0.126 cm^2, PINE Instrument Co.) and dry at room temperature for 12 h. Therefore, the catalyst loading on GC electrodes is 0.379 mg cm^{-2}. The same loading was used for the commercial IrO_2 (99.9%) and Co_3O_4 catalysts for comparison.

The CV, RDE curves were recorded in 1.0 mol L^{-1} KOH at a sweep rate of 10 mV s^{-1} between 1.00 and 1.75 V to minimize the capacitance current and evaluate the catalytic activity behavior of the film electrodes. Potentials vs. RHE were calculated by using Nernst equation $E_{RHE} = E_{Ag/AgCl} + 0.0591 * (pH) + 0.0197$ V and with the 85% iR compensation. The overpotential is given by $\eta = E_{RHE} - 1.23$ V for OER.

The stability test was measured by using amperometry J-t curve at overpotential. Electrochemical impedance spectroscopy (EIS) was recorded at open circuit potential over the frequency range between 0.01 to 10 MHz with the AC amplitude of 10 mV.

Table S1. Crystallographic data and refinement parameters for **1.**

Formula	$C_{24.33}H_{16.33}Co_{0.67}Ir_{0.67}N_2O_{5.33}P_{0.33}$
Formula Weight	599.80
T/K	123
Crystal system	hexagonal
Space Group	$P\,6_3/m$
a / Å	14.1114(19)
b / Å	14.1114(19)
c / Å	31.276(4)
Z	6
V / Å^3	5393.64(16)
d / g·cm^{-3}	1.108
F(000)	1760.0
R_{int}	0.052
T_{max} , T_{min}	0.765,0.600
Goodness-of-fit on F^2	1.004
R_1[a)],wR_2[b)][$I>2(I_0)$]	0.0474,0.1406
R_1[a)],wR_2[b)] (all data)	0.0582,0.1510
$(\Delta\rho)\text{max}, (\Delta\rho)\text{min}/\text{e Å}^{-3}$	-1.55,2.09

a) $R_1 = \sum\big||F_0| - |F_c|\big|/\sum|F_0|$

b) $\mathrm{w}R_2 = [\sum w(F_0^2 - F_c^2)^2/\sum w(F_0^2)^2]^{1/2}$

Table S2. Selected Bond Lengths (Å) and Angles (deg) for **1.**

Co1-O2	1.975(4)	P1C-P1-O4	131.20(12)
Co1-O3	1.901(6)	O4-P1-O4C	170.70(13)
Co1-O2C	1.975(5)	P1D-P1-O4	71.20(11)
Co1-O2D	1.975(5)	O3E-P1-O4	96.10(7)
O2-Co1-O3	112.62(11)	P1C-P1-C13	111.60(8)
O2-Co1-O2C	106.15(19)	O4C-P1-C13	53.40(9)
O2-Co1-O2D	112.62(12)	P1D-P1-C13	171.60(8)
O2C-Co1-O3	106.20(2)	O3E-P1-C13	115.50(4)
O2D-Co1-O3	96.10(7)	P1C-P1-O4C	58.20(8)
O2C-Co1-O2D	115.50(4)	P1C-P1-P1D	60.00(6)
O3-P1-O4	89.00(5)	P1C-P1-O3E	61.60(3)
O3-P1-C13	61.60(3)	P1D-P1-O4C	118.20(9)
P1C-P1-O3	113.4(6)	O3E-P1-O4C	89.00(5)
O3-P1-O4C	89.00(5)	P1D-P1-O3E	61.60(3)
P1D-P1-O3	61.60(3)	Co1-O2-C12	115.60(4)
O3-P1-O3E	113.4(6)	Co1-O3-P1	146.70(3)
P1-O3	1.467(7)	Co1-O3-P1C	146.70(3)
P1-O4	1.527(13)	Co1-O3-P1D	146.70(3)
P1-C13	1.799(18)	P1-O3-P1C	56.80(5)
P1-P1C	1.395(13)	P1-O3-P1D	56.80(5)
P1-O4C	1.700(3)	P1C-O3-P1D	56.80(5)
P1-P1D	1.395(140	P1-O4-P1D	50.80(7)
P1-O3E	1.467(7)	P1-O4-C13D	117.110(17)
O1-C12	1.241(9)	P1D-O4-C13D	66.30(13)
O2-C12	1.269(7)	Co1-O3-P1	146.70(3)
O4-C13D	1.580(3)	Co1-O3-P1C	146.70(3)
O3-P1-C13	117.30(13)	Co1-O3-P1D	146.70(3)

Symmetry transformations used to generate equivalent atoms:

A: -y, -1+x-y, z; B: 1-x+y, -x,z; C:1-y, x-y, z; D: 1-x+y, 1-x, z; E: x, y, 0.5-z

Table S3. The ECSA of **1**, **1@500, 1@600**, mixed- IrO_2/Co_3O_4, IrO_2, and Co_3O_4.

Catalyst	C_{dl} (mF)	m (mg)	ECSA (m^2 g^{-1})
IrO_2	3.07	0.050	153.7
1@600	1.15	0.050	57.6
1@500	0.75	0.050	37.6
Mixed-IrO_2/Co_3O_4	0.73	0.050	36.7
Co_3O_4	0.31	0.050	15.8
1	0.24	0.050	12.0

Note: The C_s value of 0.4 F m^{-2} can be used for metal oxide.[3] The loaded catalyst weight (*m*) is about 0.050 mg. The ECSA can be calculated based on equation:

$$ECSA = C_{dl} / (mC_s)$$

Table. S4 Other reported electrocatalysts for OER in 1.0 M KOH.

Catalyst	Electrolyte	Overpotential (mV) at 10mA cm^{-2}	Tafel slope (mV dec^{-1})	C_{dl} (mF cm^{-2})	Substrate	Ref.
NiCoP/C nano-boxes	1.0M KOH	300	96	146	Glassy carbon	4
Ni_2P@C	1.0M KOH	340	68	0.436	Glassy carbon	5
$CoNi_{0.5}Fe_{0.05}$-Z-H-P	1.0M KOH	329	48.2	0.017	Glassy carbon	6
CoO_x-ZIF	1.0M KOH	318	70.3	1.47	Glassy carbon	7
Co-P film	1.0M KOH	345	47	-	Cu foil	8
$Ni_{0.6}Co_{1.4}P$ nanocages	1.0M KOH	300	80	58.57	Glassy carbon	9
FeP_x/Fe-N-C/NPC	1.0M KOH	325	79	-	Glassy carbon	10
CoFe20@CC	1.0M KOH	291	58.8	2.04	Glassy carbon	11
$[NaCo(PO_3)_3]$	1.0M KOH	340	53	-	Glassy carbon	12
1@600	1.0M KOH	317.7	59.1	9.14	Glassy carbon	This work

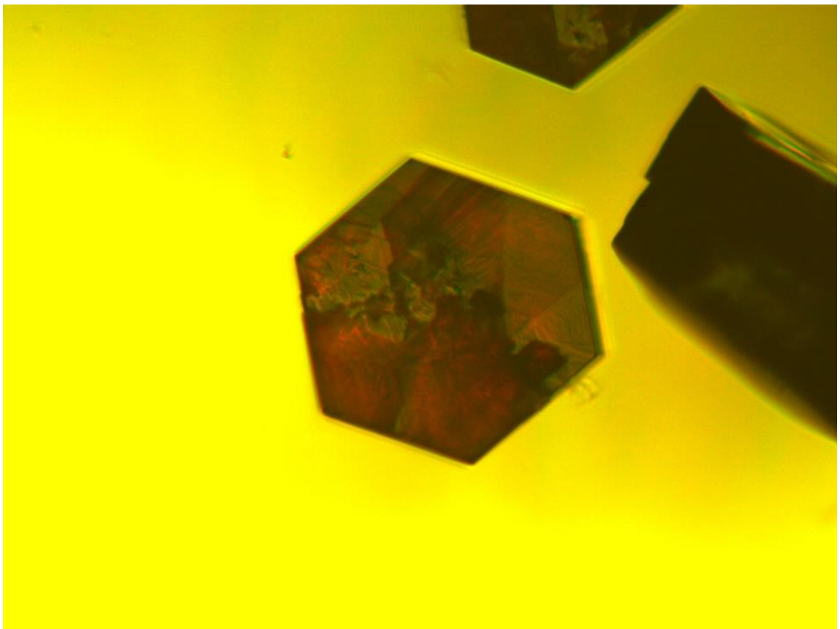

Figure S1. Microscopy image of selected crystals of **1**.

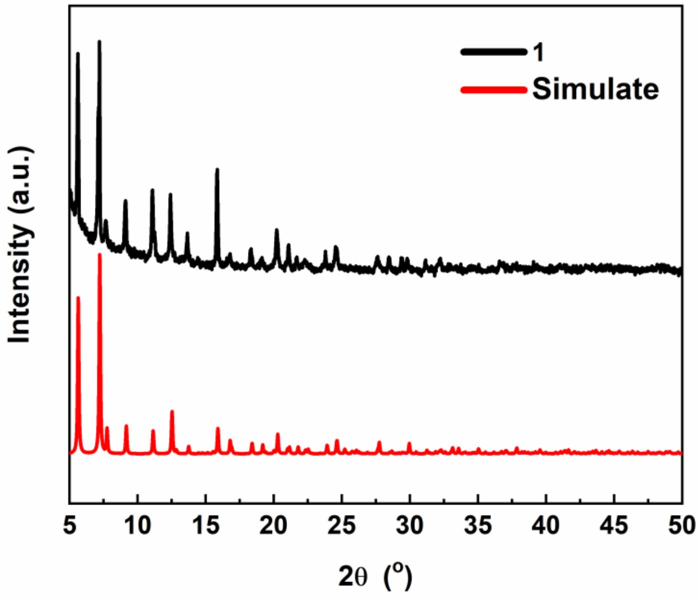

Figure S2. The PXRD pattern of **1** and that simulated from the single crystal structural data.

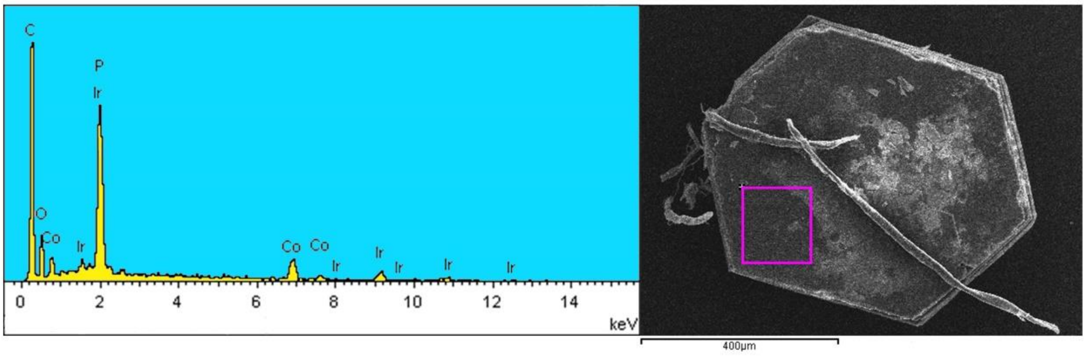

Figure S3. EDX of **1**. Atomic ratios (%): C, 79.32; O, 15.28; P: 1.44; Co, 2.15; Ir: 1.81.

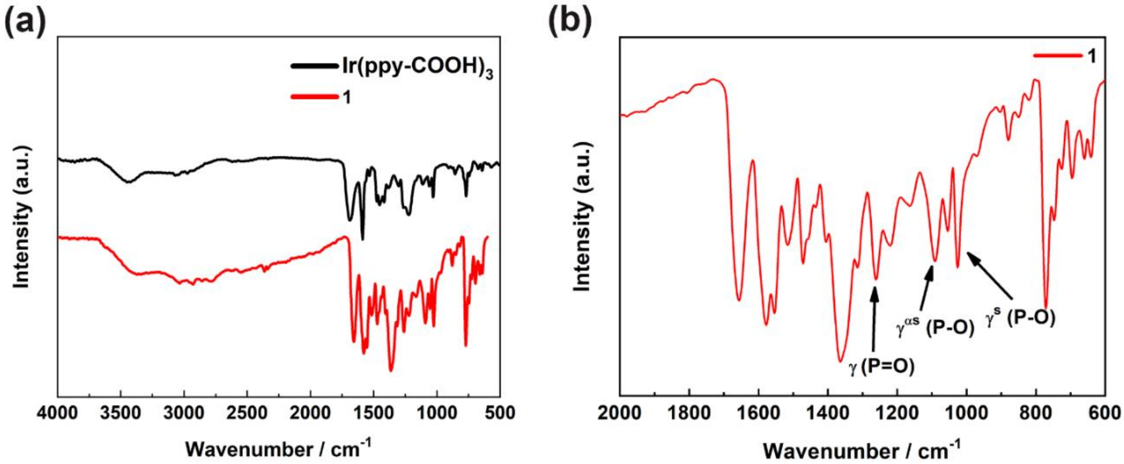

Figure S4. (a) IR spectra of **1** and ligand Ir(ppy-COOH)$_3$, (b) IR spectrum of **1** in the range 600 – 2000 cm^{-1}.

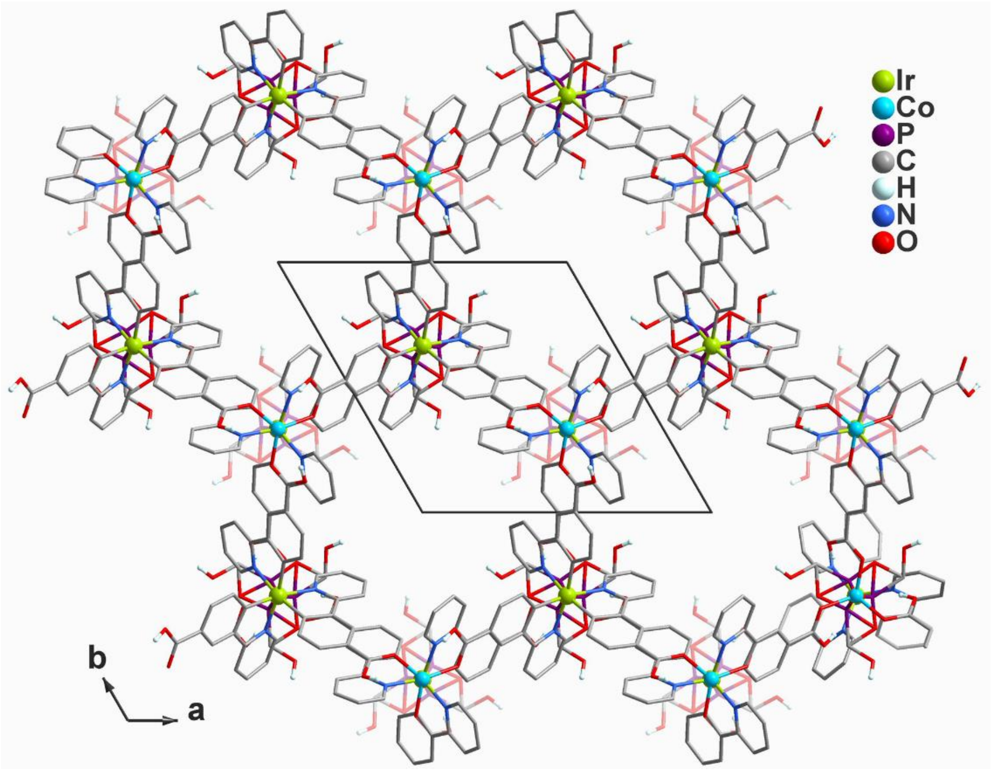

Figure S5. Packing diagram of structure **1** viewed along the *c*-axis.

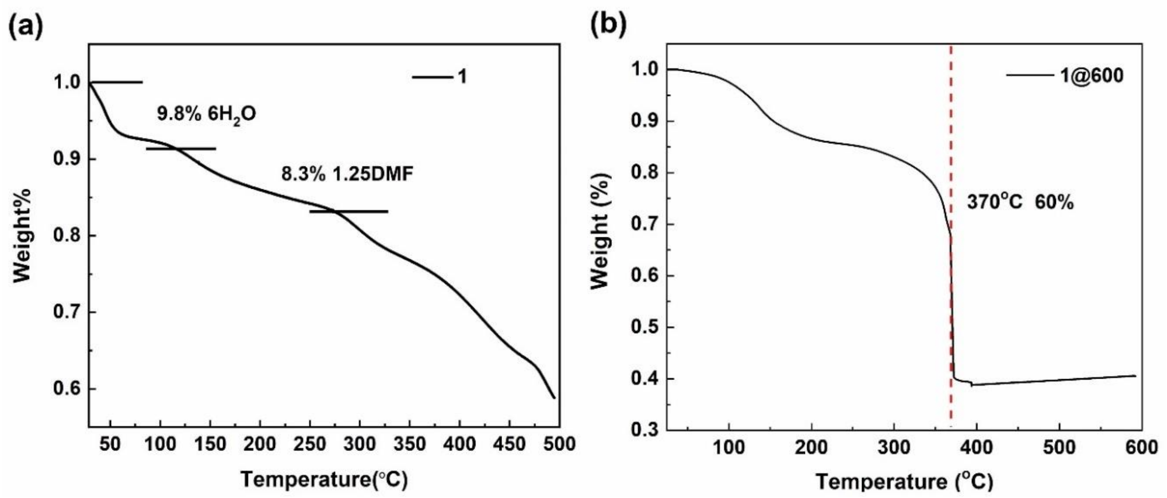

Figure S6. (a) TGA curve of **1** under N_2 flow. (b) TGA curve of **1** under O_2 flow.

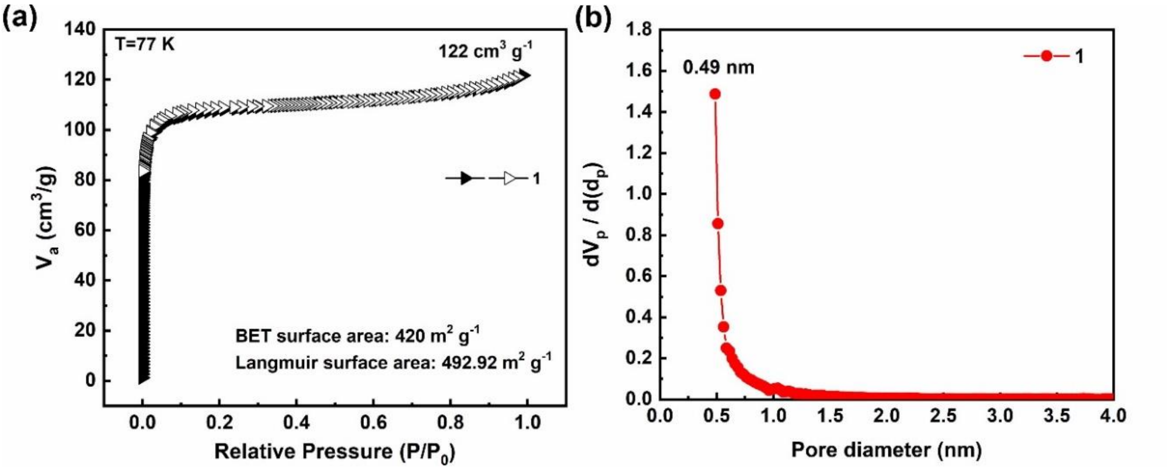

Figure S7. (a) N_2 absorption and desorption isotherm of **1** at 77 K. (b) Horvath-Kawazoe (HK) pore size distribution of **1.**

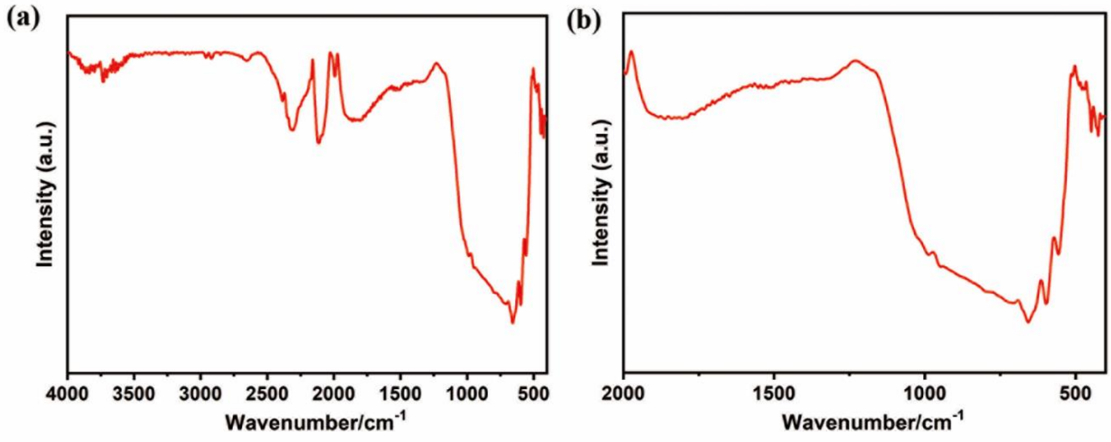

Figure S8. The IR spectrum of **1@600** in the range 400 – 4000 cm^{-1} (left) and 400 – 2000 cm^{-1} (right).

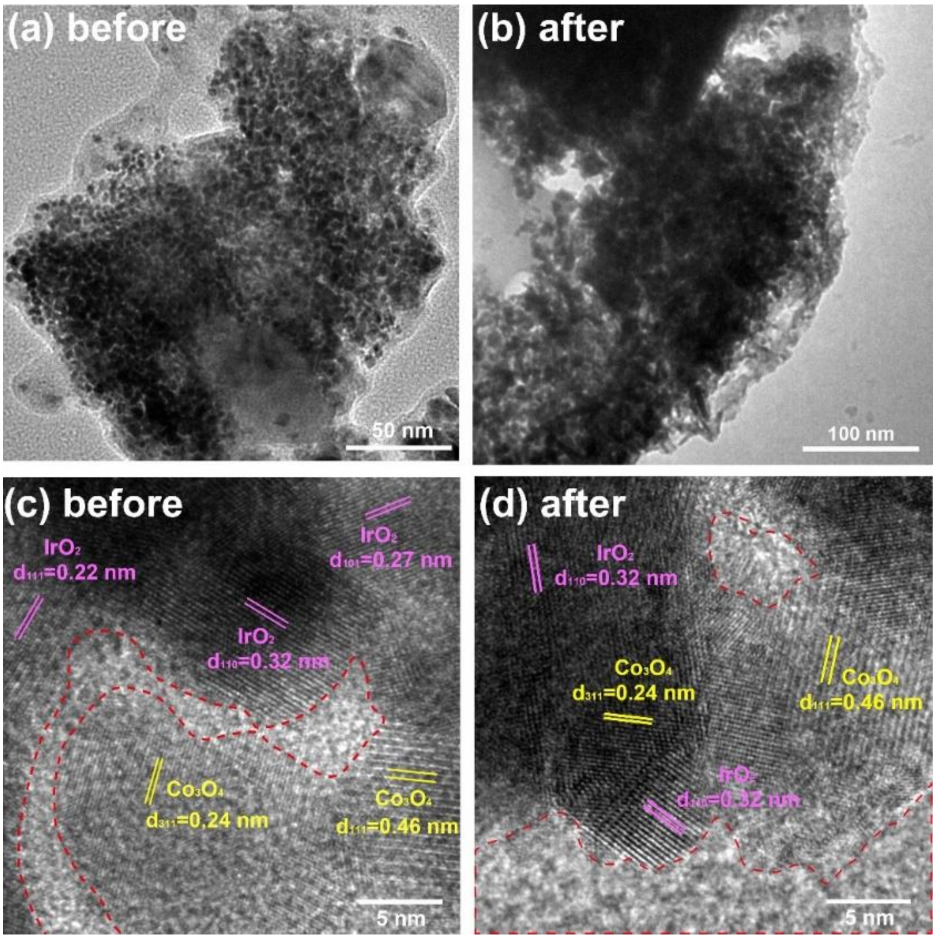

Figure S9. TEM of **1@600** (a) before, and (b) after stability test. HRTEM of **1@600** (c) before, and (d) after stability test.

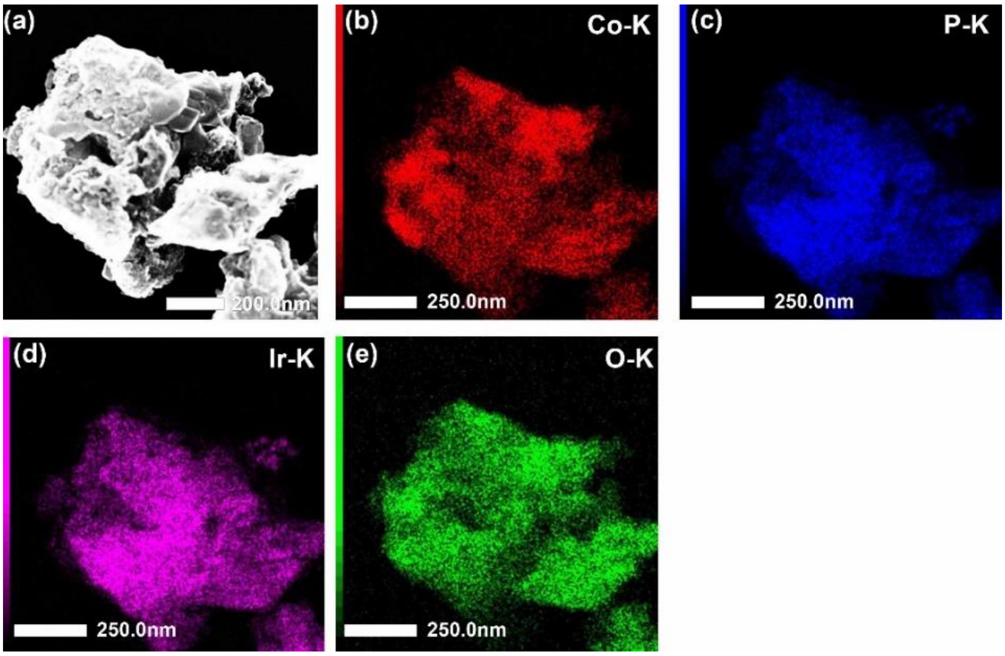

Figure S10. TEM images of (a) **1@600**. (b-e) EDX elemental mapping for Co, P, Ir, and O in **1@600**.

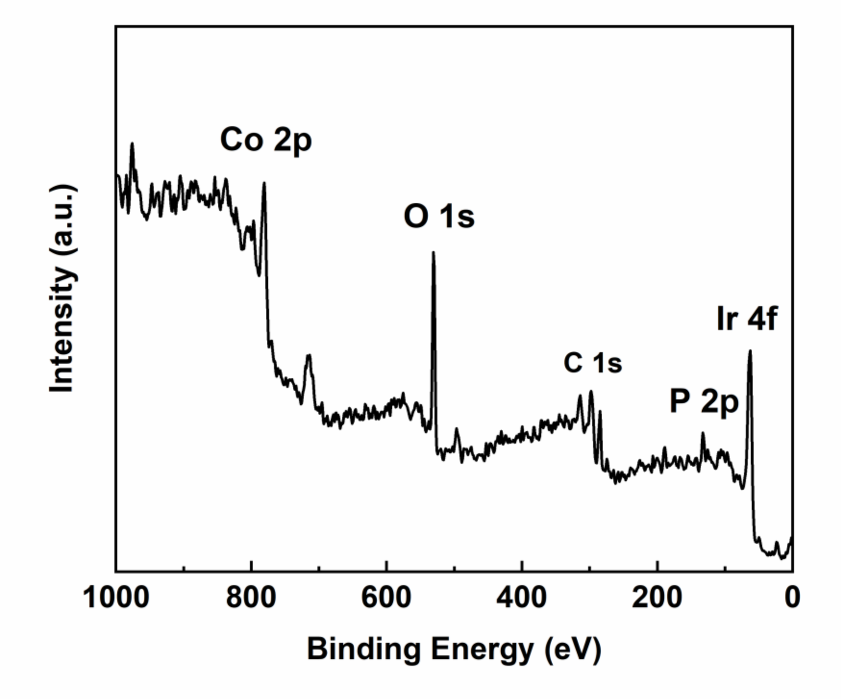

Figure S11. The XPS spectrum of **1@600**.

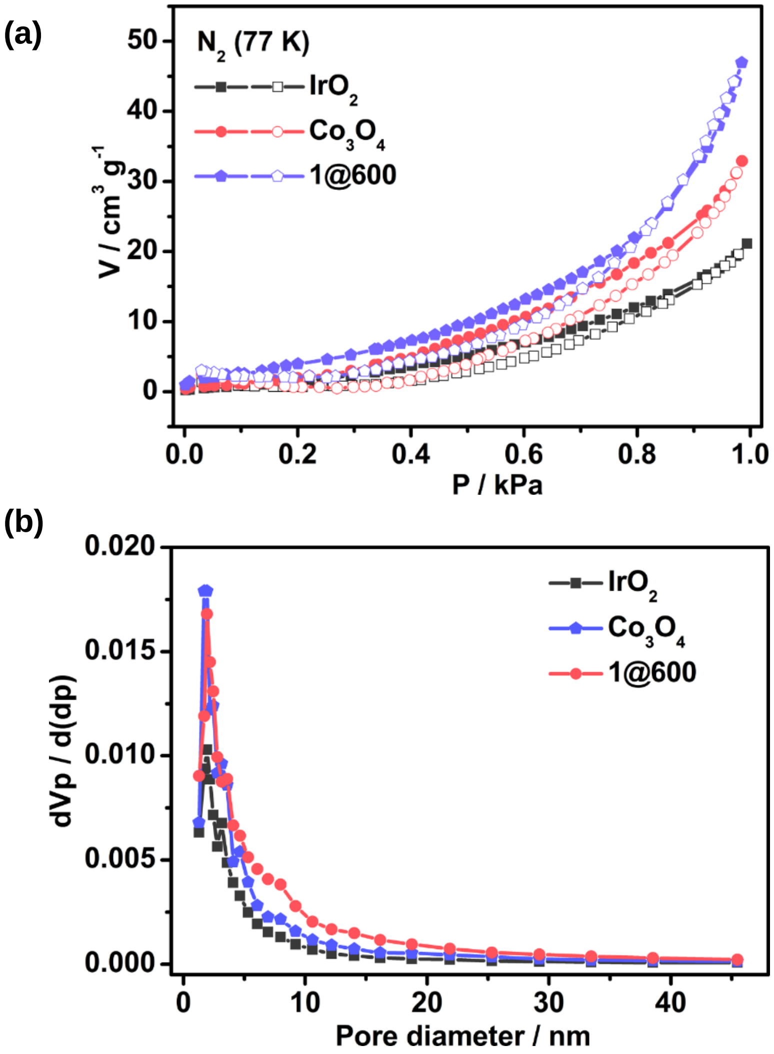

Figure S12. (a) N_2 absorption of **1@600**, and commercial IrO_2 and Co_3O_4 at 77 K. (b) Barrett-Joyner-Halenda (BJH)[13] pore size distribution of **1@600**, and commercial IrO_2 and Co_3O_4.

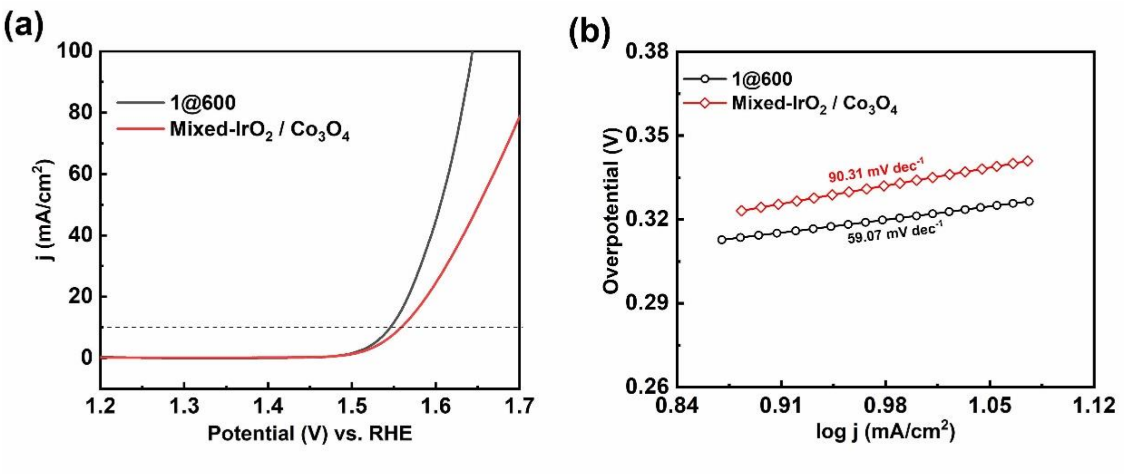

Figure S13. (a) OER polarization curve of **1@600** and mixed-IrO_2/Co_3O_4. (b) Tafel curves for **1@600** and mixed-IrO_2/Co_3O_4.

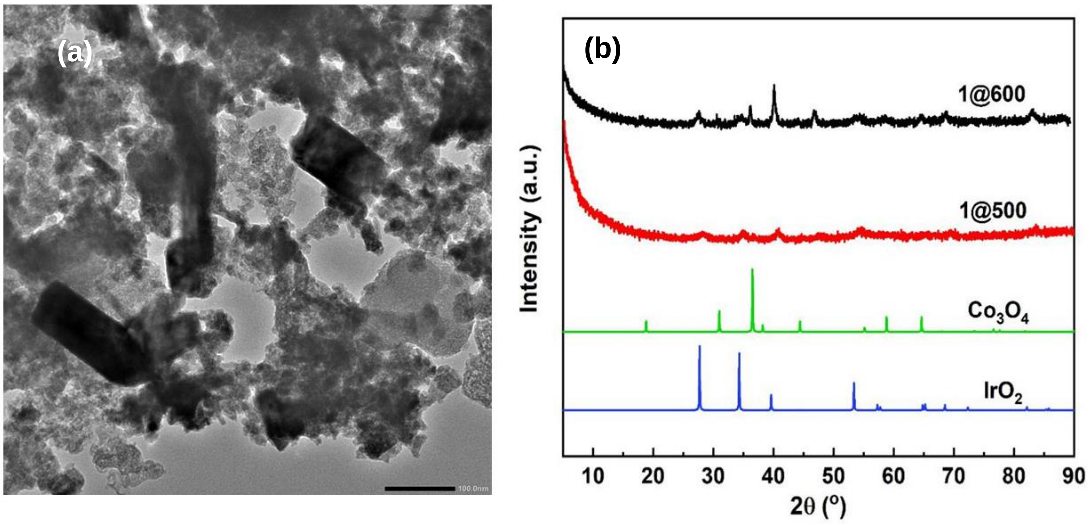

Figure S14. (a) TEM for **1@500.** (b) PXRD patterns of **1@600, 1@500,** Co_3O_4, and IrO_2.

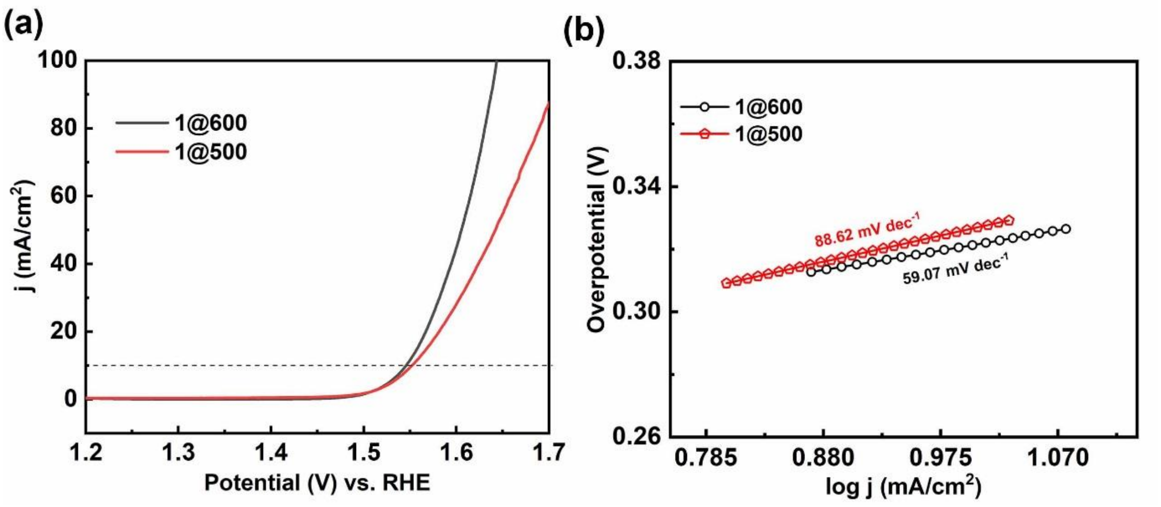

Figure S15. (a) OER polarization curves of **1@500** and **1@600.** (b) Tafel curves for **1@500** and **1@600.**

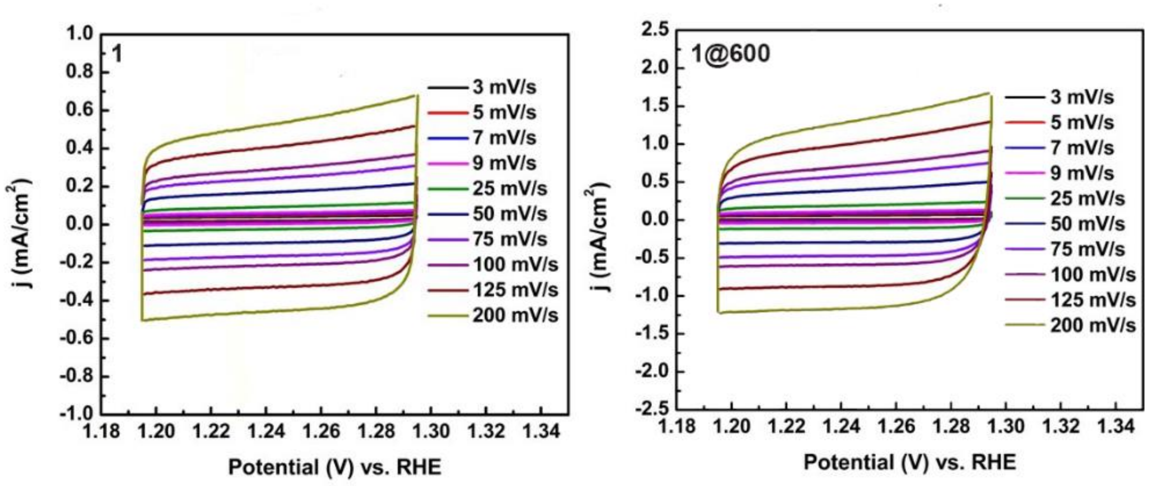

Figure S16. Cyclic voltammograms for **1** and **1@600**.

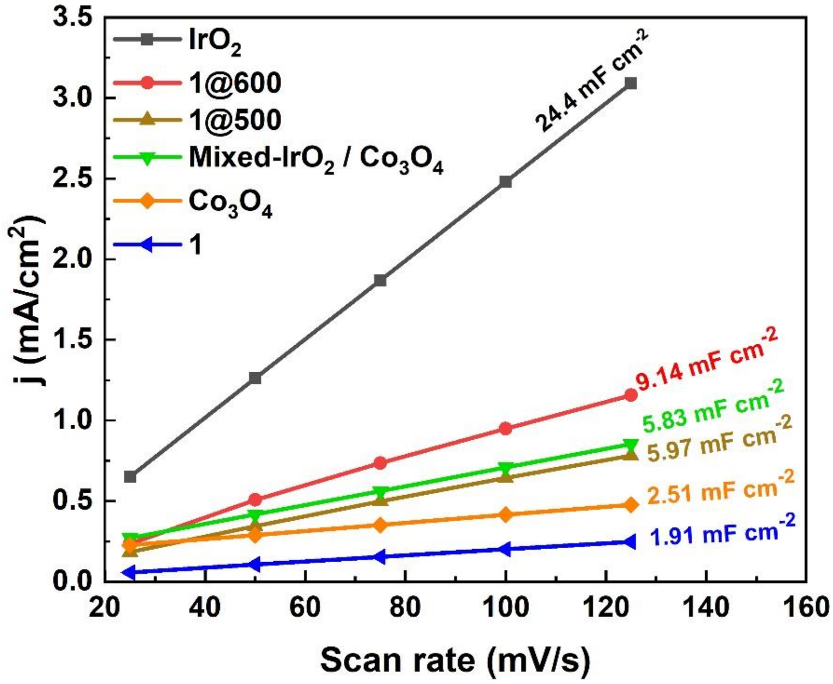

Figure S17. Double layer capacitance (C_{dl}) measurement curves for **1**, **1@500, 1@600**, mixed- IrO$_2$/Co$_3$O$_4$, IrO$_2$, and Co$_3$O$_4$.

References

1 Z. Xie, L. Ma, K. E. deKrafft, A. Jin and W. Lin*, J. Am. Chem. Soc.*, 2009, **132**, 922-923.

2 X.-G. Liu, S.-S. Bao, Y.-Z. Li and L.-M. Zheng, *Inorg. Chem.*, 2008, **47**, 5525-5527.

3 G. Li, L. Anderson, Y. Chen, M. Pan and P.-Y. A. Chuang, *Sustainable Energy Fuels,* 2018, **2**, 237-251.

4 P. He, X. Y. Yu and X. W. Lou, *Angew. Chem. Int. Ed.*, 2017, **56**, 3897-3900.

5 M. Wang, M. Lin, J. Li, L. Huang, Z. Zhuang, C. Lin, L. Zhou and L. Mai, *Chem. Commun.*, 2017, **53**, 8372-8375.

6 M. Wang, C. L. Dong, Y. C. Huang, Y. Li and S. Shen, *Small*, 2018, **14**, 1801756.

7 S. Dou, C. L. Dong, Z. Hu, Y. C. Huang, J. l. Chen, L. Tao, D. Yan, D. Chen, S. Shen and S. Chou, *Adv. Funct. Mater.,* 2017, **27**, 1702546.

8 N. Jiang, B. You, M. Sheng and Y. Sun*, Angew. Chem. Int. Ed.,* 2015, **54**, 6251-6254.

9 B. Qiu, L. Cai, Y. Wang, Z. Lin, Y. Zuo, M. Wang and Y. Chai, *Adv. Funct. Mater.,* 2018, **28**, 1706008.

10 Q. Qin, H. Jang, P. Li, B. Yuan, X. Liu and J. Cho, *Adv. Energy Mater.,* 2019, **9**, 1803312.

11 C. C. Hou, L. Zou and Q. Xu, *Adv. Mater.,* 2019, 1904689.

12 R. Gond, D. K. Singh, M. Eswaramoorthy and P. Barpanda, *Angew. Chem. Int. Ed.*, 2019, **131**, 8418-8423

13 M. Thommes, K. Kaneko, A. V. Neimark, J. P. Olivier, F. Rodriguez-Reinoso, J. Rouquerol and K. S. Sing, *Pure Appl. Chem.,* 2015, **87**, 1051-1069.